ALADIN is required for the production of fertile mouse oocytes

Sara Carvalhal[a,†,‡,*], Michelle Stevense[b,†], Katrin Koehler[c], Ronald Naumann[d], Angela Huebner[c], Rolf Jessberger[b], and Eric R. Griffis[a,§,*]

[a]Centre for Gene Regulation and Expression, School of Life Sciences, University of Dundee, Dundee DD1 5EH, United Kingdom; [b]Institute of Physiological Chemistry, Medical Faculty Carl Gustav Carus, and [c]Department of Paediatrics, University Hospital Carl Gustav Carus, Technische Universität Dresden, 01307 Dresden, Germany; [d]Max Planck Institute of Molecular Cell Biology and Genetics, 01307 Dresden, Germany

ABSTRACT **Asymmetric cell divisions depend on the precise placement of the spindle apparatus. In mammalian oocytes, spindles assemble close to the cell's center, but chromosome segregation takes place at the cell periphery where half of the chromosomes are expelled into small, nondeveloping polar bodies at anaphase. By dividing so asymmetrically, most of the cytoplasmic content within the oocyte is preserved, which is critical for successful fertilization and early development. Recently we determined that the nucleoporin ALADIN participates in spindle assembly in somatic cells, and we have also shown that female mice homozygously null for ALADIN are sterile. In this study we show that this protein is involved in specific meiotic stages, including meiotic resumption, spindle assembly, and spindle positioning. In the absence of ALADIN, polar body extrusion is compromised due to problems in spindle orientation and anchoring at the first meiotic anaphase. ALADIN null oocytes that mature far enough to be fertilized in vitro are unable to support embryonic development beyond the two-cell stage. Overall, we find that ALADIN is critical for oocyte maturation and appears to be far more essential for this process than for somatic cell divisions.**

Monitoring Editor
Yixian Zheng
Carnegie Institution

Received: Mar 11, 2016
Revised: Jun 27, 2017
Accepted: Jul 27, 2017

This article was published online ahead of print in MBoC in Press (http://www.molbiolcell.org/cgi/doi/10.1091/mbc.E16-03-0158) on August 2, 2017.

†These authors contributed equally to this work.

The authors declare that they have no conflict of interest.

Author contributions: S.C., E.R.G., M.S., and R.J. designed the experiments. S.C. and M.S. performed the experiments, analyzed the data, and cowrote the manuscript with E.R.G. K.K. performed all mouse genotyping and helped with fixed imaging. R.N. together with K.K. helped in IVF. A.H. and R.J. contributed tools and reagents. K.K., A.H., and R.J. contributed toward the manuscript.

Present addresses: ‡Instituto Gulbenkian de Ciência, 2780-156 Oeiras, Portugal; §National Institute of Neurological Disease and Stroke, National Institutes of Health, Bethesda, MD 20892.

*Address correspondence to: Eric R. Griffis (eric.griffis@nih.gov) or Sara Carvalhal (scarvalhal@igc.gulbenkian.pt).

Abbreviations used: ALADIN, alacrima-achalasia-adrenal insufficiency neurologic disorder; GFP, green gluorescent protein; GV, germinal vesicle; GVBD, germinal Vvesicle breakdown; H2B, histone H2B; MPF, maturation promoting factor; NEBD, nuclear envelope breakdown; PB, polar body; RFP, red fluorescent protein.

INTRODUCTION

Accurate chromosome segregation during mitotic and meiotic cell division is largely dependent on the proper assembly and orientation of a microtubule spindle (McNally, 2013; Ohkura, 2015; Bennabi *et al.*, 2016; di Pietro *et al.*, 2016). Spindle orientation determines where division takes place and, consequently, the size of the daughter cells (McNally, 2013). In the large majority of animal cells, the spindle is located at the center of the cell, and after division, two daughter cells of equal size are generated. Most asymmetric cell divisions are produced by displacing the spindle toward one side of the cell. Ooctyes have an extreme version of asymmetric spindle positioning (Brunet and Maro, 2007; Fabritius *et al.*, 2011). During meiosis I, the spindle assembles in the middle of the cell, but then it migrates toward the cortex. Once one of the spindle poles reaches the cortex, the spindle rotates and adopts a perpendicular orientation relative to the cortex (Fabritius *et al.*, 2011; McNally, 2013). This event marks anaphase onset, where chromosomes are extruded into a small, nondeveloping polar body (Fabritius *et al.*, 2011; McNally, 2013). This extremely asymmetric division is essential for fertilization and successful early embryonic divisions as it

preserves almost all the cytoplasmic content within the oocyte (Fabritius *et al.*, 2011; Chaigne *et al.*, 2012).

In somatic cells, interactions between polar microtubules and the cortex regulate spindle positioning. Oocytes, however, lack centrosomes and polar microtubules to interact with the cortex, and the large size of oocytes relative to the spindle also makes it difficult for microtubules to interact with the cortex. Oocyte meiotic spindles therefore rely on an alternative-positioning pathway based on the actin cytoskeleton and RanGTP, the chromosome passenger complex, and Augmin pathway (Verlhac *et al.*, 2000; Dumont *et al.*, 2007; Schuh and Ellenberg, 2008; Yi and Li, 2012; Bennabi *et al.*, 2016). How these pathways, and yet-to-be-found ones, govern spindle assembly and positioning during oocyte maturation is still not fully understood (Brunet and Maro, 2007; Fabritius *et al.*, 2011; Chaigne *et al.*, 2012; Howe and FitzHarris, 2013; McNally, 2013; Bennabi *et al.*, 2016).

Infertility affects at least 10% of couples, and between 20 and 30% of the cases are caused by failures in meiosis (Martin-du Pan and Campana, 1993; Lilford *et al.*, 1994; Yeste *et al.*, 2016). Thus it is imperative to identify novel meiotic factors and to understand their roles, which was the motivation for this study. Mice homozygous for a deletion of the *Aaas* gene are viable and males are fertile; however, null females are sterile (Huebner *et al.*, 2006), suggesting that its gene product ALADIN could be required for oocyte maturation and production of functional female gametes.

Aaas was first identified as the gene that is mutated in triple A syndrome, and later it was shown that the ALADIN protein is a component of the nuclear pore complex (NPC), which regulates nucleocytoplasmic transport (Tullio-Pelet *et al.*, 2000; Handschug *et al.*, 2001; Cronshaw *et al.*, 2002). ALADIN mutations cause defects in the nuclear import of DNA repair proteins and ferritin during interphase (Hirano *et al.*, 2006; Storr *et al.*, 2009; Prasad *et al.*, 2013; Juhlen *et al.*, 2015). Studies in human cells have now uncovered ALADIN's role in spindle assembly via the spatial regulation of Aurora A kinase (Carvalhal *et al.*, 2015). We showed that during mitosis ALADIN localizes around the spindle, and its depletion slows spindle assembly, weakens the spindle, and reduces spindle length; potentially due to the mislocalization of known Aurora A substrates involved in spindle assembly and maintenance (Carvalhal *et al.*, 2015). Given the essential role of spindles in meiosis, we examined the role of ALADIN in meiotic spindle formation and behavior.

Here we show that ALADIN is essential for proper meiotic spindle assembly and positioning during meiosis in mouse oocytes, leading to catastrophic failures in the first meiotic divisions for most oocytes. We also show that the few ALADIN null oocytes that can be fertilized in vitro cannot support embryonic development beyond the two-cell stage, demonstrating that this protein is essential for producing fertile eggs.

RESULTS AND DISCUSSION

ALADIN's localization is conserved during meiosis in mouse oocytes

During interphase, ALADIN is localized at the nuclear pore complex (Cronshaw *et al.*, 2002). In mitotic human cells, ALADIN localizes around the mitotic spindle and enriches at spindle poles. To test whether ALADIN's localization is conserved in female meiosis, we fixed wild-type germinal vesicle (GV)-stage oocytes and stained them with an ALADIN-specific antibody (Supplemental Figure S1A, top panel). ALADIN was found to be enriched at the nuclear membrane as expected and absent from oocytes obtained from homozygous ALADIN knockout (*Aaas*$^{-/-}$) mice (Supplemental Figure S1A). We then analyzed ALADIN's localization throughout meiotic progression. Wild-type (WT) oocytes from prometaphase I until metaphase II were fixed and stained for ALADIN and tubulin (Figure 1A). During prometaphase, the nuclear envelope disassembles, and a ring of ALADIN staining was found around the condensing chromosomes. As the spindle forms in metaphase I, ALADIN was localized to the periphery of the spindle, as previously described in mitotic somatic cells (Carvalhal *et al.*, 2015). However, ALADIN's localization at the spindle poles observed in somatic cells was seen in oocytes only when more stringent fixative conditions were used (Supplemental Figure S1B). ALADIN remained around the spindle as it moved toward the cortex. The ALADIN intensity around the spindle appeared to be reduced as the oocytes underwent anaphase, but it reappeared around the second spindle by metaphase II.

To confirm ALADIN's localization, we injected WT oocytes with capped mRNAs encoding GFP–ALADIN and H2B-RFP and imaged developing oocytes up to metaphase I. Before nuclear envelope breakdown (NEBD), GFP–ALADIN was localized at the nuclear membrane (GV; nucleus, Figure 1B, left panel). When chromosomes were fully condensed and aligned at the metaphase plate, ALADIN was localized around the aligned chromosomes in a distribution that was similar to the ALADIN staining described above (Figure 1B, right panel). The presence of GFP–ALADIN was also observed in clusters throughout the cytoplasm, potentially a result of the overexpressed protein aggregating or incorporating into annulate lamellae (Figure 1B). Together these results suggest a conservation of ALADIN's localization around the spindle in somatic and germ cells.

Interestingly, we found that the injection of a high concentration of ALADIN mRNA impairs GV breakdown (GVBD; Figure 2A). Injection of low levels of ALADIN mRNA into wild-type oocytes did not affect the timing of GVBD, but injection with twice the amount of mRNA resulted in 24 of the 49 oocytes failing to undergo GVBD 6 h after meiosis resumption. However, the oocytes injected with the higher levels of mRNA that did undergo GVBD did so with a timing that was similar to what was seen in control oocytes or oocytes injected with 45% less ALADIN mRNA. This binary response to the injection of high levels of ALADIN mRNA is consistent with an all-or-nothing defect in meiotic resumption rather than a specific defect in GVBD. This suggests that an overabundance of ALADIN can have a dominant negative effect in meiosis. Although the involvement of ALADIN at NEBD in somatic cells has not yet been determined, ALADIN is tethered to the NPC by the transmembrane nucleoporin (NUP) NDC1 (Kind *et al.*, 2009; Yamazumi *et al.*, 2009), which is required for NPC assembly in vertebrate cells (Haren *et al.*, 2006; Mansfeld *et al.*, 2006; Stavru *et al.*, 2006). Therefore we cannot exclude the possibility that ALADIN affects GVBD indirectly through altering NDC1 function or the nuclear import of maturation promoting factors (MPFs), which triggers GVBD. Alternatively, Aurora A has been shown to have a role in the initiation of meiosis in oocytes (Saskova *et al.*, 2008), and we have shown that the overexpression of ALADIN can inhibit Aurora A's centrosomal activity in somatic cells (Carvalhal *et al.*, 2015). Therefore it is also possible that the overabundance of ALADIN could halt meiotic initiation and GVBD by reducing Aurora A activity at this stage.

Deletion of ALADIN disturbs oocyte maturation in vitro

We next tested whether a lack of ALADIN could affect meiosis. ALADIN female homozygous knockout mice (*Aaas*$^{-/-}$) are viable but sterile. Histological sections of ovaries from wild-type and ALADIN-deficient mice did not show any differences, and follicular development and ovulation appeared to be normal (Huebner *et al.*, 2006). Therefore we decided to analyze whether this infertility could be a consequence of ALADIN having a role in meiosis. WT (*Aaas*$^{+/+}$) and *Aaas*$^{-/-}$ oocytes were collected and maintained in a prophase arrest

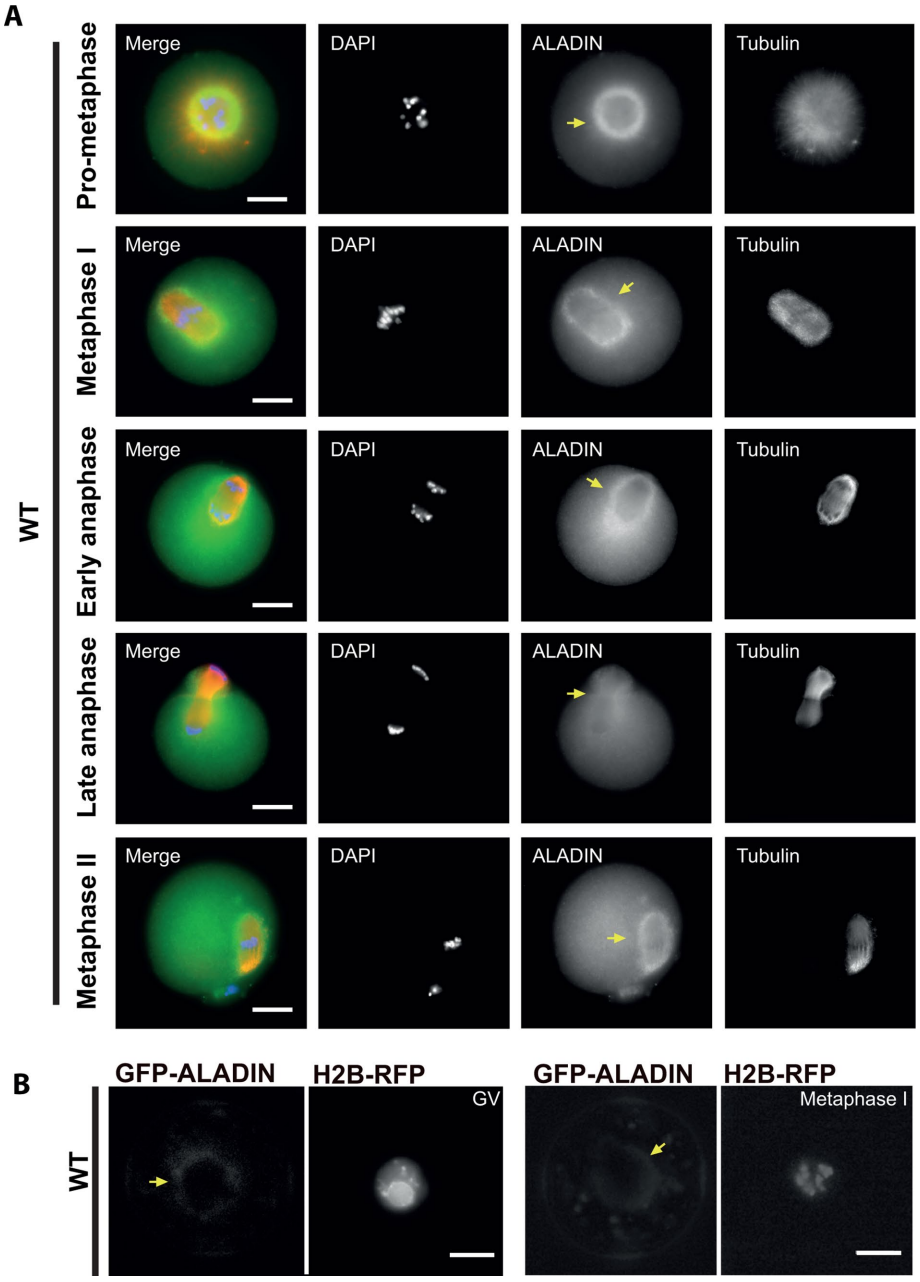

FIGURE 1: ALADIN localizes around the meiotic spindle during mouse oocyte maturation. (A) Wild-type oocytes at various stages of meiotic progression were fixed and immunostained for ALADIN and α-tubulin and then costained with DAPI. Representative wide-field fluorescence images from a single z-plane are shown. Scale bar = 50 μm. (B) Live imaging performed with wild-type mouse oocytes expressing GFP–ALADIN and H2B-RFP. Single Z-stack frames are presented from representative oocytes at germinal vesicle (GV) stage (left panel) and at metaphase I (right panel). Scale bar = 20 μm. Yellow arrows indicate ALADIN's localization, which was observed in more than three independent experiments.

by incubation in media with milrinone. Oocytes were released from milrinone, and their progression through meiosis was monitored by bright-field imaging. One and a half hours after meiotic resumption, 90% of the 102 WT oocytes progressed past GVBD, but only 59% of 105 *Aaas*$^{-/-}$ oocytes did so. On average, ALADIN-deficient oocytes required significantly longer to undergo GVBD (Figure 2B; WT: 1.9 h ± 1.3 vs. *Aaas*$^{-/-}$: 2.7 h ± 1.6; ***$p < 0.001$). Fifteen hours after GVBD, 80% of WT oocytes extruded their first polar body (PB). In contrast, only 50% of *Aaas*$^{-/-}$ oocytes extruded a polar body, which increased to 57% 18 h after GVBD (Figure 2C). This process was also significantly slower in the *Aaas*$^{-/-}$ than the WT (WT: 9.6 h ± 2.8 vs. *Aaas*$^{-/-}$: 11 h ± 2.5; **$p < 0.007$).

ALADIN is required for correct spindle positioning in asymmetric oocyte divisions

So far we had observed that the absence of ALADIN slows both GVBD and PB extrusion timing and hinders the extrusion of PBs in oocytes. Our ALADIN depletion studies in somatic cells found that this protein is required for the timing of spindle assembly and formation of spindles of the proper length (Carvalhal *et al.*, 2015). As ALADIN's localization is conserved around the spindle in both cell models, we next tested whether ALADIN could also participate in spindle assembly during oocyte cell division. Meiotic spindle assembly with and without ALADIN was analyzed by time-lapse fluorescence imaging of microtubules (marked by GFP–β-tubulin) and chromosomes (marked by H2B-RFP) after injection with capped mRNAs (Supplemental Movie S1). As before, injected *Aaas*$^{-/-}$ oocytes took longer to achieve GVBD (Figure 2D) and had a reduced ability to extrude polar bodies. In contrast to the bright-field imaging that was done before, we did notice more polar body ejection failures in the wild-type cells when performing fluorescence imaging, but the general trends of increased meiotic difficulties in *Aaas*$^{-/-}$ oocytes remained. Representative frames of this imaging are shown in Figure 3, which includes a representative example of a *Aaas*$^{-/-}$ oocyte that successfully extruded its PB (middle column) and another that failed to remain anchored at the cortex at anaphase I (right column).

On average, *Aaas*$^{-/-}$ oocytes took 96 min longer than wild-type oocytes to assemble a bipolar metaphase spindle after GVBD (Figure 4A; 3.0 h ± 1.9 vs. 4.6 h ± 3.2; **$p < 0.05$). Also, these bipolar structures were significantly shorter (Figure 4C; 8.3% shorter; **$p < 0.05$) when compared with WT spindles. Both observations are in agreement with depletion of ALADIN in somatic cells (Carvalhal *et al.*, 2015). Without ALADIN, Aurora A kinase spreads from centrosomes onto somatic mitotic spindle microtubules, affecting the distribution of a subset of microtubule regulators, slowing spindle assembly and chromosome alignment. When we examined the localization of Aurora A and active Aurora A in oocytes, we could not see any evident spread of Aurora A onto *Aaas*$^{-/-}$ meiotic spindles (Supplemental Figure S2, A and B). However, we cannot rule out that *Aaas*$^{-/-}$ oocytes have subtle changes in HURP (hepatoma up-regulated protein) or Augmin localization within the meiotic spindle; both of these proteins are known to be involved in acentriolar spindle assembly and maintenance (Breuer *et al.*, 2010; Colombie

A

Condition	GVBD	No GVBD
Positive Control (no injection)	87% (n=26)	13% (n=4)
Control (H2B-RFP)	86% (n=24)	14% (n=4)
Lower ALADIN expression (GFP-ALADIN + H2B-RFP)	81% (n=13)	19% (n=3)
Higher ALADIN expression (GFP-ALADIN + H2B-RFP)	51% (n=25)	49% (n=24)

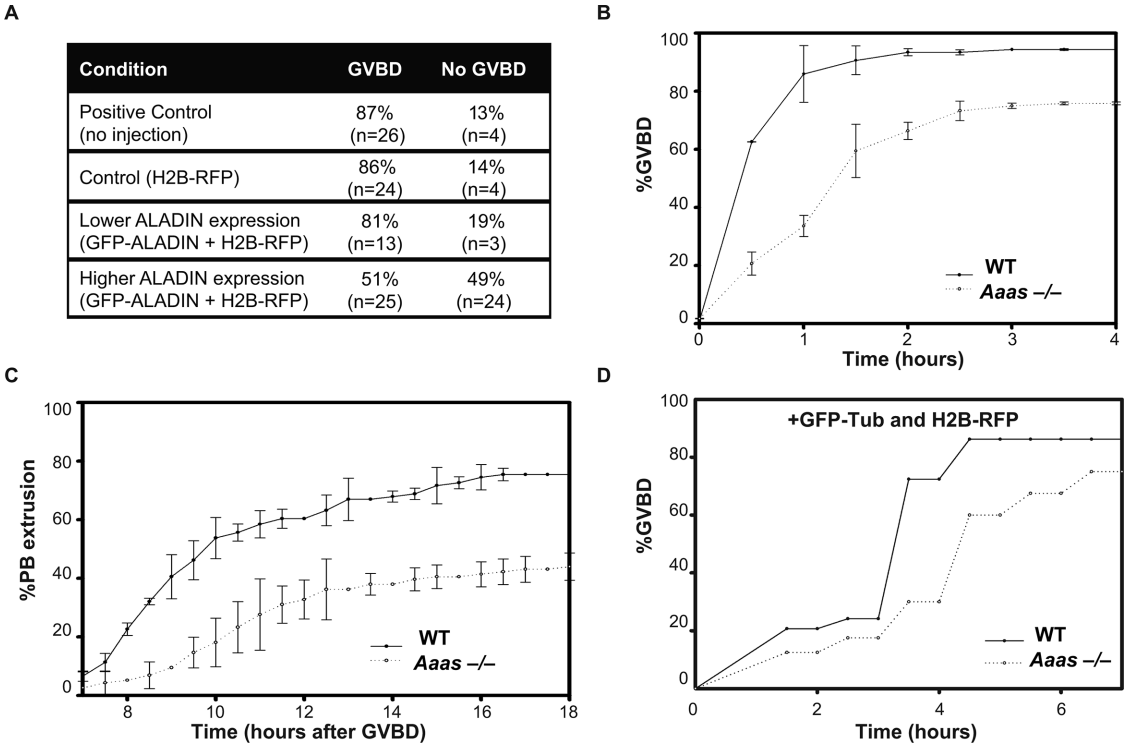

FIGURE 2: ALADIN levels are important for proper GVBD and polar-body extrusion. (A) Wild-type oocytes were injected with the indicated mRNAs and the cumulative percentage of GVBD was measured over time. Uninjected oocytes were used as the positive control, and all the remaining conditions were injected with similar volumes of capped mRNAs. To express lower levels of ALADIN, oocytes were injected with a GFP–ALADIN mRNA 45% less concentrated (4.4 μg/μl) than in the higher expression (8 μg/μl) condition. The table shows the percentage of these oocytes that underwent GVBD. n indicates the number of oocytes measured in each condition. GVBD mean time ± SD for Control: 2.2 ± 0.5 h; H2B-RFP: 2.4 ± 1.1 h; lower expression of GFP–ALADIN + H2B-RFP: 2.3 ± 0.4 h and higher expression of GFP–ALADIN + H2B-RFP: 2.62 ± 1.0 h. All experiments were performed at least three times with the exception of lower expression of GFP–ALADIN + H2B-RFP (n = 1, result from oocytes collected from two mice). (B) Cumulative percentage of GVBD and corresponding SD over time in WT and *Aaas*$^{-/-}$ oocytes. More than 100 oocytes from five independent experiments were collected and measured for each condition evaluated. The average time for GVBD of WT oocytes was 1.9 ± 1.3 h while *Aaas*$^{-/-}$ oocytes took significantly longer to achieve GVBD (2.7 ± 1.6 h, ***$p < 0.001$). (C) Cumulative percentage of first polar body extrusion and corresponding SD over time in WT and *Aaas*$^{-/-}$ oocytes. Results from more than three independent experiments. Mean ± SD: 9.6 ± 2.8 h vs. 11 ± 2.5 h; **$p < 0.007$. (D) Cumulative percentage of GVBD in WT (control) and *Aaas*$^{-/-}$ oocytes expressing GFP–β-tubulin and H2B-RFP.

et al., 2013). Although these processes share common pathways, we have to consider that meiotic spindles are not just mitotic spindles without centrosomes, and several pathways are likely regulated in a meiosis-specific manner, suggesting that ALADIN may have distinct roles in meiosis that differ from the ones already uncovered in mitosis.

Asymmetric positioning of meiotic spindles allows for the expulsion of chromosomes into small, nondeveloping polar bodies (Fabritius *et al.*, 2011; McNally, 2013). To examine spindle relocation from the center of the oocyte to the cortex, we measured the time from spindle bipolarization to first contact with the cortex (Figure 4, B and D). ALADIN null oocytes showed a slower and more variable migration of the spindle to the cortex, when compared with WT oocytes (Figure 4D; 2.8 h ± 1.2 vs. 3.5 h ± 2.7).

Before anaphase, spindles attach by one pole to the oocyte cortex. To analyze how spindles approached the cortex, we measured the angle formed between the spindle pole and the cell periphery (θ; Figure 4, B and E) when it first interacted with the cortex. We sorted these data for cells that could extrude a polar body (PBE) or for those that could not (NO PBE). In wild-type conditions, independent of their success in extruding polar bodies (PBE and NO PBE), spindles consistently arrived at the oocyte cortex at a defined angle (Figure 4E, 122.3° ± 11.8 and 122.5° ± 9.6, respectively, and Supplemental Movie S1). However, in the case of the *Aaas*$^{-/-}$ oocytes, we noticed differences in how the spindle approached the cortex (Supplemental Movie S2). In *Aaas*$^{-/-}$ ooctyes that ejected a polar body, the spindles approached the cortex at an angle that was similar to what is seen in wild-type oocytes (113.1° ± 19.9, 14 oocytes). In *Aaas*$^{-/-}$ oocytes that failed polar body ejection, we observed a highly variable angle of approach between the spindle pole and the cortex (110.3° ± 48.4, 17 oocytes). Figure 3 and Supplemental Movie S2 show examples of *Aaas*$^{-/-}$ oocytes that ejected (center oocyte in Figure 3 and left oocyte in Supplemental Movie S2) and did not eject a polar body (right oocyte in Figure 3 and right oocyte in Supplemental Movie S2). In these oocytes, we observed that the spindle can approach the cortex in an oblique, looping manner, but polar body ejection can proceed normally, while the spindle within the oocyte can approach the cortex in a very direct manner but fail to anchor to the cortex for polar body ejection. We often observed that the spindle

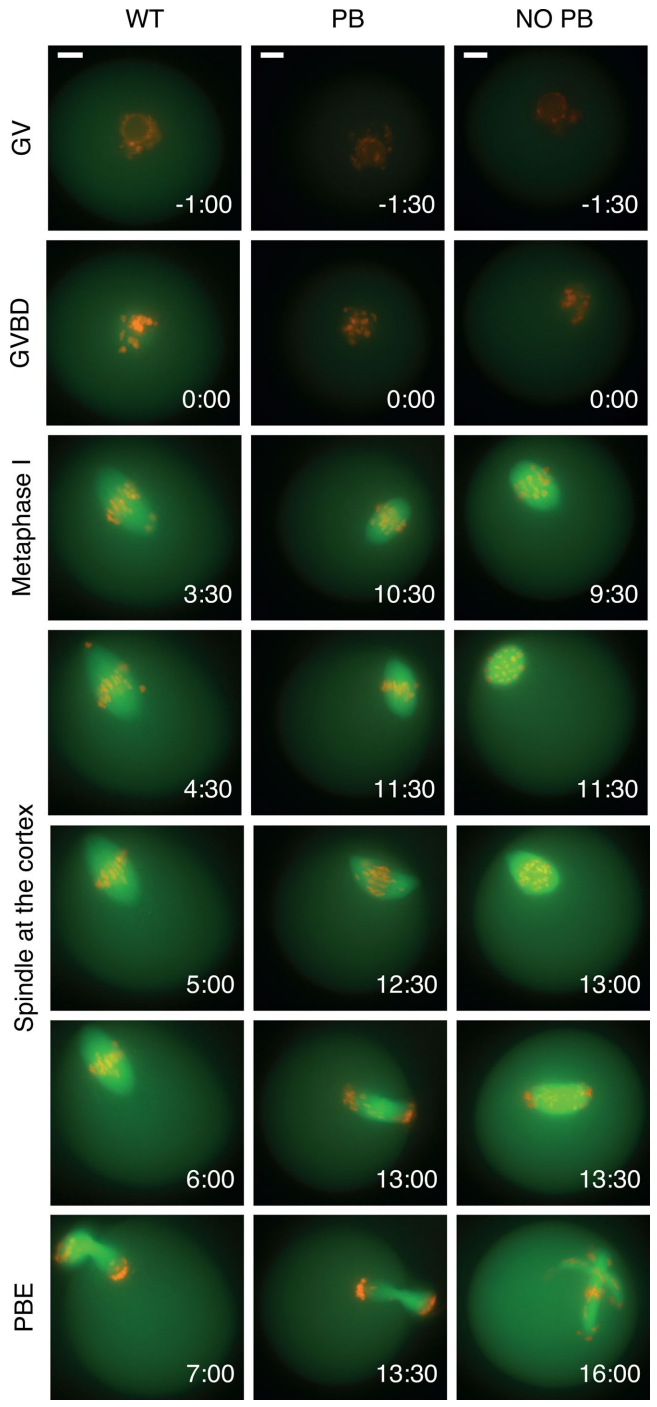

FIGURE 3: Oocytes lacking ALADIN show impaired spindle positioning and have less robust spindles. Time-lapse analysis of progression through the first meiotic division in control (WT, left column) and *Aaas*$^{-/-}$ oocytes expressing GFP–β-tubulin and H2B-RFP. Middle column shows a representative *Aaas*$^{-/-}$ oocyte that was able to extrude a polar body. The right column shows a representative *Aaas*$^{-/-}$ oocyte that fails to extrude a polar body. Representative still frames presented. Time 0:00 represents GVBD in hours:minutes. GV, germinal vesicle; GVBD, germinal vesicle breakdown; and PBE, polar body extrusion. Scale bars = 20 μm.

migrates to the cortex and initiates anaphase but it is not maintained in that position. Therefore anaphase completes in the center of the cell and polar body extrusion fails (Figure 3, right, and Supplemental Movie S2, right). These results suggest that ALADIN is required for both stereotypical spindle migration as well as the maintenance and/or formation of proper connections between the spindle and the oocyte cortex. In mouse oocytes, spindle positioning and rotation is known to be driven by a cytoplasmic actin network (Dumont *et al.*, 2007; Schuh and Ellenberg, 2008; Yi and Li, 2012). No relationship between ALADIN and actin has been published so far, but ALADIN is localized around the spindle, where actin nucleation occurs and convection forces are generated (Grill *et al.*, 2001; Bezanilla and Wadsworth, 2009). A matrix or envelope has been observed to assemble around the spindle in many different systems. This structure is composed of nucleoporins, lamins, and vesicles from the Golgi and ER and has been proposed to function as a nonmicrotubule scaffold able to concentrate spindle assembly factors, tether force generators, and stabilize the spindle (Zheng, 2010; Jiang *et al.*, 2014, 2015a,b; Schweizer *et al.*, 2014, 2015). Many nuclear pore proteins were identified by mass spectrometric analysis of purified *Xenopus* spindle matrices (Ma *et al.*, 2009). When we consider ALADIN's localization around the spindle and ability to interact with other NUPs, we think that it is reasonable to hypothesize that ALADIN could be a member of this matrix with a role in promoting spindle migration, rotation, and/or anchoring in the oocyte.

ALADIN is essential for the production of fertile eggs

Our results suggest that *Aaas*$^{-/-}$ oocytes fail PB extrusion due to severe problems in the asymmetric positioning of the meiotic spindle relative to the oocyte cortex. However, some ALADIN null cells did successfully eject a PB, and so we tested whether these oocytes were able to support fertilization and embryonic maturation.

We counted the homologues and chromosomes present in oocytes before and after PB ejection in chromosome spreads from wild-type and *Aaas*$^{-/-}$ oocytes. Normal complements of chromosomes with grossly typical structures were found in both conditions; we counted 20 homologues in all six metaphase I oocytes observed and 20 chromatids in two metaphase II *Aaas*$^{-/-}$ oocytes (Figure 4F and *data not shown*). These results reinforced the finding that some oocytes lacking ALADIN progress to a point where they can be fertilized.

To determine whether these oocytes can be fertilized and support embryogenesis, we performed in vitro fertilization (IVF) experiments (Figure 5 and Supplemental Figure S1C). On day 0 (IVF day), WT (C57Bl6N/Crl) spermatozoa were used to fertilize Black6 control (C57Bl6N/Crl), wild-type (*Aaas*$^{+/+}$), or *Aaas*$^{-/-}$ in vivo matured metaphase II oocytes (Figure 5). We measured the fertilization rate by calculating the percentage of two-cell stage embryos present on day 1, from the total number of oocytes used in the IVF experiment after superovulation on day 0. In both WT strains the fertilization rate was high; 37.3% (Black6 control) and 35.0% (*Aaas*$^{+/+}$) of the oocytes were able to form two-cell embryos (Figure 5B, far left graph). These numbers are comparable to routine fertilization rates achieved in our mouse transgenic facility. In contrast, the *Aaas*$^{-/-}$ cells had a reduced fertilization rate of 11.4%. The two-cell stage embryos were allowed to develop until day 4 (Figure 5A), where we observed healthy blastocysts in both WT strains (Black6 control; 28.9%, *Aaas*$^{+/+}$; 24.3%), confirming the success of IVF in forming quality embryos. However, the *Aaas*$^{-/-}$ embryos were unable to progress past the two-cell stage (0.0% blastocyst formation). This incapacity to progress further than the two-cell stage was observed in independent experiments (Supplemental Figure S1C). These results suggest that although some *Aaas*$^{-/-}$ oocytes are able to properly segregate their chromosomes in meiosis I, only a small portion of these cells can be fertilized (Figure 5:

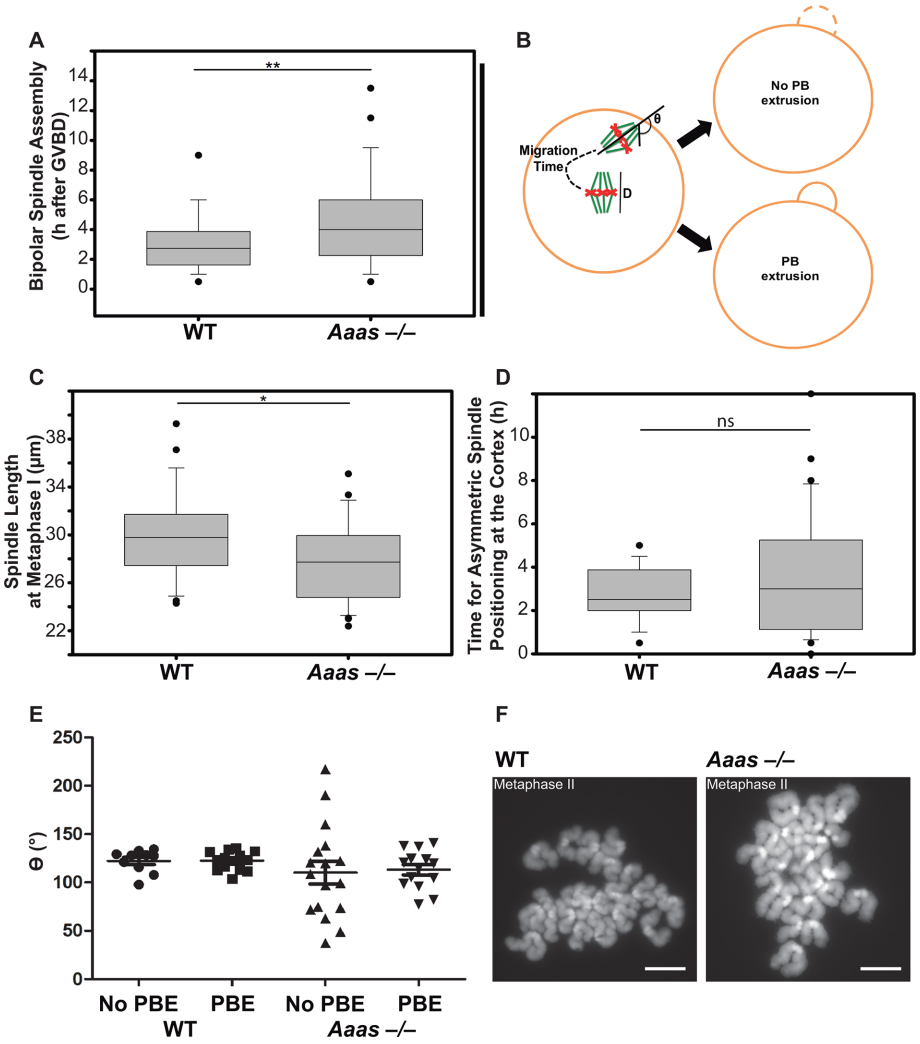

FIGURE 4: ALADIN is required for correct spindle assembly and positioning in oocyte meiosis. (A) The time from GVBD to bipolar spindle assembly was measured in 24 control (WT) and 29 *Aaas*$^{-/-}$ oocytes expressing GFP–β-tubulin and H2B-RFP. *Aaas*$^{-/-}$ oocytes formed spindles more slowly and showed greater variability in spindle assembly timing (3.0 ± 1.9 h vs. 4.6 ± 3.2 h; $^{**}p < 0.005$). Bipolar spindle assembly was scored as the time when two individual poles were distinguishable. (B) Explanatory diagram of the measurements reported in C–E. The pole-pole distance, D, of metaphase I spindles were measured when bipolar spindles structures have a compact and organized metaphase plate. The black dotted line represents the migration time from the assembly of metaphase I spindles to the point when spindles contact the oocyte cortex. θ represents the angle made between the spindle interacting with the cortex and a line that crosses both spindle poles and the cortex. (C) Box-plot showing metaphase I spindle length in WT and *Aaas*$^{-/-}$ oocytes expressing GFP–β-tubulin and H2B-RFP. *Aaas*$^{-/-}$ oocytes have a shorter spindle in metaphase; 29.9 ± 3.6 µm *vs.* 27.5 ± 3.3 µm, $^{*}p < 0.05$. (D) The migration time of the spindle, as explained in B, was measured for the indicated conditions (2.8 ± 1.2 h *vs.* 3.5 ± 2.7 h). ns = nonsignificant. (E) The cortex angle represented as θ and explained in B was measured and the measurements are reported for oocytes that extruded a polar body (designated as PBE) and oocytes that failed to extrude their polar body after reaching the cortex (NO PBE). WT PBE: 122.3° ± 11.8 from 14 oocyte measured, WT NO PBE: 122.5° ± 9.6 (10 oocytes), *Aaas*$^{-/-}$ PBE: 113.1° ± 19.9 (14 oocytes), and *Aaas*$^{-/-}$ NO PBE: 110.3° ± 48.4 (17 oocytes). All figures represent the results obtained from the analysis of four independent experiments executed with similar concentrations of GFP–β-tubulin and H2B-RFP mRNAs ([C and D] WT = 24 and *Aaas*$^{-/-}$ = 31 oocytes analyzed). (F) Representative metaphase II chromosome spreads of WT and *Aaas*$^{-/-}$ oocytes are presented. ALADIN deletion does not affect chromosome segregation after PB extrusion, since 20 sister chromatids are present in metaphase II. It also does not affect chromosome structure or sister chromatid pairing. Box-and-whisker plot: Middle line shows the median value; the bottom and top of the box show the lower and upper quartiles (25–75%); whiskers extend to the 10th and 90th percentiles, and all outliers are shown. $^{*}p < 0.05$, $^{**}p < 0.005$, and ns = nonsignificant after *t* test analysis. Scale bars = 10 µm.

11.4%, Supplemental Figure S1C: 6.3%). However, of the few oocytes that were fertilized, none were able to progress further than the two-cell stage without ALADIN (Figure 5: 0.0%, Supplemental Figure S1C: 0.0%), explaining why these mice are infertile.

Therefore we can hypothesize that the lack of ALADIN compromises the quality of mature oocytes, as they were unable to successfully develop into blastocyst embryos. However, at this point we cannot exclude that ALADIN has additional roles in meiosis II or in the first mitotic division.

In conclusion, the female infertility seen in mice lacking ALADIN is caused by multiple defects in oocyte maturation, revealing a new role of ALADIN in meiosis. Some oocytes can tolerate these perturbations and mature to the point where they can be fertilized, but the *Aaas*$^{-/-}$ eggs are then incapable of supporting early embryogenesis. Mutations of ALADIN are known to cause triple A syndrome (Huebner *et al.*, 2000; Tullio-Pelet *et al.*, 2000; Handschug *et al.*, 2001; Sarathi and Shah, 2010). The majority of these patients develop their symptoms during early childhood and fertility defects in these patients have never been closely analyzed. Female mice that express only the S263P mutant variant of ALADIN are fertile (data not shown), suggesting that this mutant still retains some function in meiosis, which is consistent with our finding that cells from patients expressing only this variant have spindle assembly defects that are not as extreme as those seen in the Q387X variant expressing cells (Carvalhal *et al.*, 2015). Interestingly, the *Aaas*$^{-/-}$ mice show no defects in male fertility, suggesting that ALADIN plays a particularly important role in asymmetric and acentrosomal divisions. Our current data do not allow us to determine whether this is due to the fact that acentrosomal oocytes utilize an alternative spindle assembly and/or anaphase division pathway that relies more heavily on ALADIN or whether ALADIN is required for the proper preparation of the oocyte prior to the resumption of meiosis I. However, given that the acute depletion of ALADIN in somatic cells produces mechanical defects in spindle function and we also see defects in meiotic progression after ALADIN is overexpressed, we favor the former hypothesis.

MATERIALS AND METHODS

Mouse oocyte and sperm collection and culture

C57BL/6 background WT (*Aaas*$^{+/+}$) and *Aaas*$^{-/-}$ were previously described (Huebner *et al.*, 2006). Together with the WT

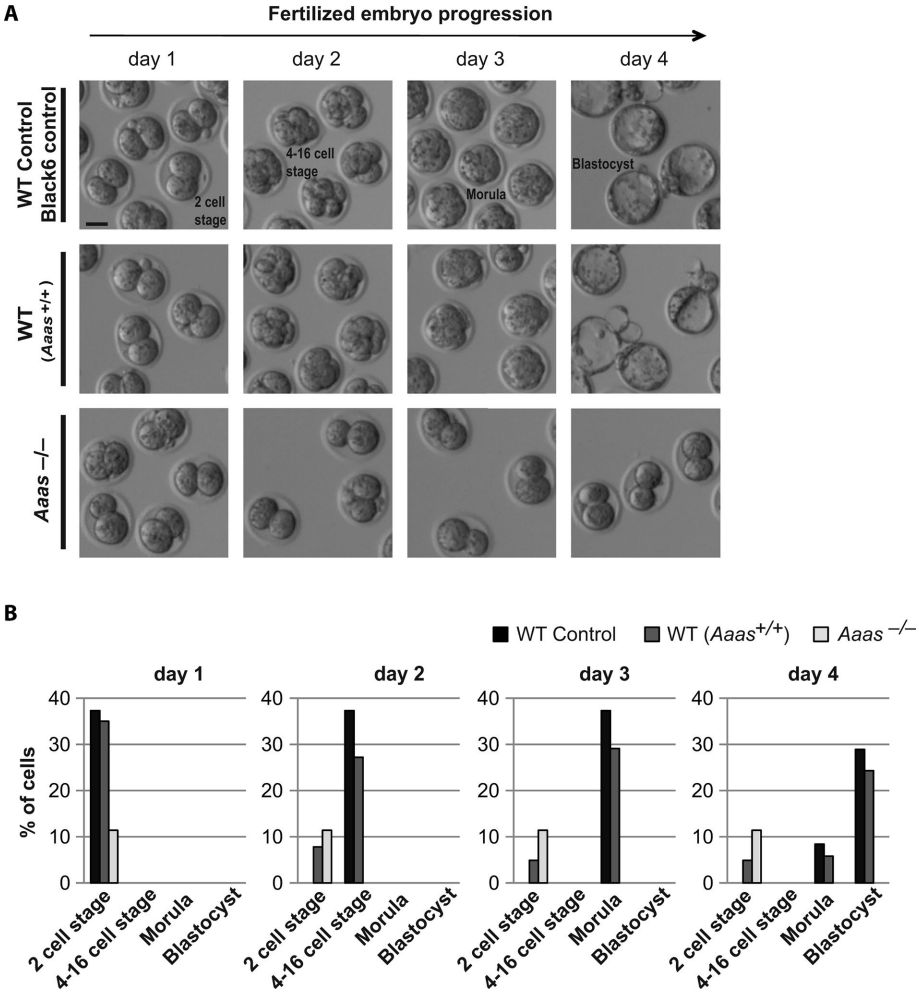

FIGURE 5: *Aaas*$^{-/-}$ oocytes cannot support early embryogenesis. (A) Black6 control, *Aaas*$^{+/+}$ and *Aaas*$^{-/-}$ mice were used to perform in vitro fertilization (IVF). The oocytes were collected after superovulation and fertilized using wild-type (Black6) spermatozoa (day 0). On day 1, the fertilized two-cell stage cells were counted, separated, and imaged until day 4. Scale bar = 50 µm. (B) The percentages of 2-cell and 4- to 16-cell morula and blastocyst stage embryos (of the total number of embryos isolated after superovulation) are shown for each day.

strain 129SvEMS mice used in immunofluorescence experiments, these animals were bred and maintained under pathogen-free conditions at the Experimental Center of the Medizinisch-Theoretisches Zentrum of the Medical Faculty at the Dresden University of Technology according to approved animal welfare guidelines. WT strain C57Bl/6NCrl (Black6 control) mice used in the IVF experiment were bred and maintained under pathogen-free conditions at the Biomedical Services Facility of the MPI-CBG according to approved animal welfare guidelines.

Oocytes were isolated from adult mice by puncturing the ovaries with needles in M2 medium supplemented with 2.5 µM milrinone to ensure prophase arrest. Surrounding follicular cells were removed by mouth pipetting. Resumption of oocyte maturation was induced by washing out the milrinone. For immunofluorescence analysis oocytes were incubated in preequilibrated M2 media covered by paraffin oil and incubated at 37°C until the desired stage (metaphase I: 6–7 h, metaphase II: 12–13 h). Female mice between 2 and 10 mo of age were used (knockout and control mice of similar ages were always used in the same assay to eliminate potential confounding effects of maternal age).

In vitro transcription, microinjections, live oocyte imaging, and quantitative analysis

GFP–β-tubulin, histone H2B-RFP, and GFP–ALADIN mRNAs were synthesized with the T3 mMessage mMachine Kit (Ambion) according to the manufacturer's instructions and purified using LiCl Precipitation (Ambion) or RNAeasy columns (Qiagen). The plasmids pRN3–GFP–β-tubulin and pRN3-histone H2B-RFP were a gift from K. Wassmann (CNRS, Paris, France; Touati *et al.*, 2012). Human GFP–ALADIN was cloned into pRN3E (gift from K. Wassmann) with *Xho*I and *Bam*HI and mRNA was transcribed and purified as above.

Oocytes arrested in prophase were injected using a FemtoJet microinjector (Eppendorf) with constant flow settings. To allow expression of fusion proteins and oocyte recovery, oocytes were incubated for 3–6 h in media supplemented with milrinone. After release into M2 medium, oocytes were imaged every 30 min for up to 30 h on an inverted Nikon TE2000E microscope with a Plan APO 40 ×/1.25 NA objective or Plan APO 63 ×/1.4 NA objective, a CoolSNAP HQ camera (Photometrics), standard filter sets, and with an environmental chamber to maintain 37° C. Z-series optical stacks of 80 µm were recorded with slices taken every 7 µm. For analysis of GVBD and polar body extrusion of noninjected oocytes, a Plan APO 20 ×/0.75 NA objective was used. All images were acquired using the Nikon NIS-Elements ND2 software.

Quantitative time-lapse data were analyzed manually using NIS-Elements software. Metaphase I time was defined when bipolar spindles structures have the most compact and organized metaphase plate. At this stage, pole-to-pole length of the spindle was measured using the tubulin signal. To calculate the migration of the spindle to the cortex, the time when one spindle pole reached the oocyte cortex was compared with the corresponding metaphase I timing. At this time, the angle made by the converging spindle pole with the cortex and spindle structure was measured.

Immunofluorescence microscopy, quantitative analysis, and antibodies used

Oocytes were cultured in M2 plus or minus 2.5 µM milrinone and collected at the relevant time points. The zona pellucida was removed using tyrode's solution (T1788; Sigma). After a 30-min recovery period, the oocytes were fixed in 2% formaldehyde and 0.1% Triton X-100 in M2 media for 10 mins. Cells were washed once in blocking buffer (5% bovine serum albumin [BSA] and 0.1% Triton X-100 in phosphate-buffered saline [PBS]), before incubation in blocking buffer for 1–2 h at room temperature (RT). The cells were transferred into the primary antibody solution and incubated at 4°C overnight. Primary antibodies used were as follows: mouse anti-ALADIN 5A1 (H00008086-M02; Abnova) at 1:100 rat anti-tubulin alpha (MCA78G; Bio-Rad) at 1:10,000, mouse anti–α-tubulin

(Abcam; ab11316), rabbit anti–Aurora A (Abcam; ab2254) at 1:200, and rabbit anti–phospho-Aurora A (T288; Abcam; ab58494) at 1:200 all in 2% BSA in PBS. The cells were washed at RT in 2% BSA in PBS 3 × 5 min and transferred to the secondary antibody solution for 1–2 h at RT. Secondary antibodies used were as follows: goat anti-mouse immunoglobulin G (IgG) Alexa Fluor 488 (A-11001; Invitogen) at 1:2000, goat anti-rabbit Cy3 (Invitrogen; A10520) at 1:2000, and goat anti-rat IgG Alexa Fluor 568 (A-11077; Invitrogen) at 1:2000 in 0.5% BSA in PBS. The cells were washed at RT in 0.5% BSA in PBS 3 × 5 min and mounted in Vectashield (H-1000; Vector Laboratories) plus 1 µg/ml DAPI (4′,6-diamidino-2-phenylindole) for imaging. A single 40× magnification z-plane image in each channel was acquired on a wide-field fluorescence Zeiss Axiophot upright microscope. When strong fixation was used, oocytes were fixed in 0.1% Triton X-100, 0.2% glutaraldehyde, 2% paraformaldehyde (PFA) diluted in 1× PHEM buffer (60 mM 1,4-piperazinediethanesulfonic acid [PIPES], 25 mM *N*-(2-hydroxyethyl)piperazine-*N*′-(2-ethanesulfonic acid) [HEPES], 10 mM ethylene glycol-bis(2-aminoethylether)-*N*,*N*,*N*′,*N*′-tetraacetic acid [EGTA], and 2 mM $MgCl_2$, pH 6.9) for 14 h at 4° C. Oocytes were attached to Superfrost Plus Microscope Slides (Fisher Scientific) and incubated for 10 min in PHEM + 0.1% Triton X-100 three times prior to permeabilization (1% Triton 1× PHEM for 30 min) and blocking (3% BSA, 0.05% Tween 20 in 1× PHEM for 30 min). All the remaining staining was performed as described in Carvalhal *et al.* (2015). Rat anti–α-tubulin (Pierce) was used at 1:200, and mouse anti-ALADIN (3E9; Santa Cruz) at 1:50 was used to confirm the staining seen with the other anti-ALADIN antibody. Secondary antibodies were highly cross-subtracted Alexa Fluor 488, -555, conjugated anti-mouse, and -rat used at 1:200 (Life Technologies). DAPI at 2 µg/ml was used to stain chromosomal DNA. Fixed oocytes were imaged in a Leica SP2 confocal microscope. Representative images are shown. Images may be modified in min/max intensity for presentation but never in γ (γ = 1.0).

Chromosome spreads

Chromosome spreads were prepared according to an adapted method from Hodges and Hunt (2002). Briefly, the zona pellucida of oocytes arrested at metaphases I and II was removed using acid treatment (Tyrodes solution; Sigma) and oocytes were transferred onto one well of a 10-well glass slide into 15 µl of fixation solution (1% PFA, 0.1% Triton X-100, 3 mM DTT; pH 9.2). After drying for several hours at room temperature, slides were washed 3 × 5 min in PBS and then mounted with Vectashield (Vector Laboratories) containing 1 µg/ml DAPI (Sigma). Images were captured under oil using 100× magnification.

In vitro fertilization

For IVF experiments, ampulla from super ovulated mice were dissected from the oviduct and the cumulus-oocyte complexes released (day 0). Surrounding follicular cells were removed using hyaluronidase treatment. The zona was perforated with a 600-µs pulse of a 1460-nm laser set at 63% power at room temperature (Hamilton Thorne). The spermatozoa were activated in capacitation media. Concentration and motility of fresh spermatozoa was evaluated and only spermatozoa with standard qualities were used. The cells were incubated together for 4 h at 37°C in HTF (human tubal fluid) media to allow fertilization to occur. After incubation, the oocytes were washed once in potassium-supplemented simplex optimized medium (KSOM) to remove spermatozoa and cumulus cells and then transferred to preequilibrated KSOM under paraffin oil for culture at 37°C. The fertilization status of each oocyte was assessed by the presence of pronuclei 10 h after the beginning of the insemination. After overnight culture of the oocytes, the fertilized and developed two-cell stage cells were counted, separated, and imaged at 5× magnification until day 4. The embryos were transferred to fresh preequilibrated KSOM under oil each day.

Statistical analysis and data representation

Data obtained from NIS-Elements software were imported into Sigma-plot software (Systat Software), which was used to generate box-and-whisker and cumulative distribution plots, with the exception of the one shown in Figures 2, B and C, and 4E (GraphPad Prism). In box-and-whisker plots the middle line shows the median value; the bottom and top of the box show the lower and upper quartiles; whiskers extend to the 10th and 90th percentiles, and all outliers are shown. Student's *t* test was used to determine statistical significance between two different treatments (significance is reported in each figure). Images represented were produced in Illustrator, FIJI, and OMERO WebFigure.

ACKNOWLEDGMENTS

We thank Katja Wassmann for plasmids and Attila Toth for discussion. We thank the Light Microscopy Facility, College of Life Sciences, University of Dundee, for help with imaging. M.S. is supported through institutional funds and DFG (Deutsche Forschungsgemeinschaft) grant STE-2280/2-1, and A.H. and K.K. are supported by DFG grants HU-895/5-1 and HU-895/5-2. S.C. was supported by an EMBO Short Term Fellowship (ASTF-521-2014) and a Biotechnology and Biological Sciences Research Council studentship. R.J. is supported by institutional funds and by DFG grant JE-150/11-2. E.R.G. was supported by a Wellcome Trust RCDF award (090064/Z/09/Z) and a Wellcome Trust Strategic award to the Centre for Gene Regulation and Expression (097945/B/11/Z).

REFERENCES

Bennabi I, Terret ME, Verlhac MH (2016). Meiotic spindle assembly and chromosome segregation in oocytes. J Cell Biol 215, 611–619.

Bezanilla M, Wadsworth P (2009). Spindle positioning: actin mediates pushing and pulling. Curr Biol 19, R168–169.

Breuer M, Kolano A, Kwon M, Li CC, Tsai TF, Pellman D, Brunet S, Verlhac MH (2010). HURP permits MTOC sorting for robust meiotic spindle bipolarity, similar to extra centrosome clustering in cancer cells. J Cell Biol 191, 1251–1260.

Brunet S, Maro B (2007). Germinal vesicle position and meiotic maturation in mouse oocyte. Reproduction 133, 1069–1072.

Carvalhal S, Ribeiro SA, Arocena M, Kasciukovic T, Temme A, Koehler K, Huebner A, Griffis ER (2015). The nucleoporin ALADIN regulates Aurora A localization to ensure robust mitotic spindle formation. Mol Biol Cell 26, 3424–3438.

Chaigne A, Verlhac MH, Terret ME (2012). Spindle positioning in mammalian oocytes. Exp Cell Res 318, 1442–1447.

Colombie N, Gluszek AA, Meireles AM, Ohkura H (2013). Meiosis-specific stable binding of augmin to acentrosomal spindle poles promotes biased microtubule assembly in oocytes. PLoS Genet 9, e1003562.

Cronshaw JM, Krutchinsky AN, Zhang W, Chait BT, Matunis MJ (2002). Proteomic analysis of the mammalian nuclear pore complex. J Cell Biol 158, 915–927.

di Pietro F, Echard A, Morin X (2016). Regulation of mitotic spindle orientation: an integrated view. EMBO Rep 17, 1106–1130.

Dumont J, Million K, Sunderland K, Rassinier P, Lim H, Leader B, Verlhac MH (2007). Formin-2 is required for spindle migration and for the late steps of cytokinesis in mouse oocytes. Dev Biol 301, 254–265.

Fabritius AS, Ellefson ML, McNally FJ (2011). Nuclear and spindle positioning during oocyte meiosis. Curr Opin Cell Biol 23, 78–84.

Grill SW, Gonczy P, Stelzer EH, Hyman AA (2001). Polarity controls forces governing asymmetric spindle positioning in the Caenorhabditis elegans embryo. Nature 409, 630–633.

Handschug K, Sperling S, Yoon SJ, Hennig S, Clark AJ, Huebner A (2001). Triple A syndrome is caused by mutations in AAAS, a new WD-repeat protein gene. Hum Mol Genet 10, 283–290.
Haren L, Remy MH, Bazin I, Callebaut I, Wright M, Merdes A (2006). NEDD1-dependent recruitment of the gamma-tubulin ring complex to the centrosome is necessary for centriole duplication and spindle assembly. J Cell Biol 172, 505–515.
Hirano M, Furiya Y, Asai H, Yasui A, Ueno S (2006). ALADINI482S causes selective failure of nuclear protein import and hypersensitivity to oxidative stress in triple A syndrome. Proc Natl Acad Sci USA 103, 2298–2303.
Hodges CA, Hunt PA (2002). Simultaneous analysis of chromosomes and chromosome-associated proteins in mammalian oocytes and embryos. Chromosoma 111, 165–169.
Howe K, FitzHarris G (2013). Recent insights into spindle function in mammalian oocytes and early embryos. Biol Reprod 89, 71.
Huebner A, Mann P, Rohde E, Kaindl AM, Witt M, Verkade P, Jakubiczka S, Menschikowski M, Stoltenburg-Didinger G, Koehler K (2006). Mice lacking the nuclear pore complex protein ALADIN show female infertility but fail to develop a phenotype resembling human triple A syndrome. Mol Cell Biol 26, 1879–1887.
Huebner A, Yoon SJ, Ozkinay F, Hilscher C, Lee H, Clark AJ, Handschug K (2000). Triple A syndrome—clinical aspects and molecular genetics. Endocr Res 26, 751–759.
Jiang H, He X, Feng D, Zhu X, Zheng Y (2015a). RanGTP aids anaphase entry through Ubr5-mediated protein turnover. J Cell Biol 211, 7–18.
Jiang H, He X, Wang S, Jia J, Wan Y, Wang Y, Zeng R, Yates J 3rd, Zhu X, Zheng Y (2014). A microtubule-associated zinc finger protein, BuGZ, regulates mitotic chromosome alignment by ensuring Bub3 stability and kinetochore targeting. Dev Cell 28, 268–281.
Jiang H, Wang S, Huang Y, He X, Cui H, Zhu X, Zheng Y (2015b). Phase transition of spindle-associated protein regulate spindle apparatus assembly. Cell 163, 108–122.
Juhlen R, Idkowiak J, Taylor AE, Kind B, Arlt W, Huebner A, Koehler K (2015). Role of ALADIN in human adrenocortical cells for oxidative stress response and steroidogenesis. PLoS One 10, e0124582.
Kind B, Koehler K, Lorenz M, Huebner A (2009). The nuclear pore complex protein ALADIN is anchored via NDC1 but not via POM121 and GP210 in the nuclear envelope. Biochem Biophys Res Commun 390, 205–210.
Lilford R, Jones AM, Bishop DT, Thornton J, Mueller R (1994). Case-control study of whether subfertility in men is familial. Bmj 309, 570–573.
Ma L, Tsai MY, Wang S, Lu B, Chen R, Iii JR, Zhu X, Zheng Y (2009). Requirement for Nudel and dynein for assembly of the lamin B spindle matrix. Nat Cell Biol 11, 247–256.
Mansfeld J, Guttinger S, Hawryluk-Gara LA, Pante N, Mall M, Galy V, Haselmann U, Muhlhausser P, Wozniak RW, Mattaj IW, *et al*. (2006). The conserved transmembrane nucleoporin NDC1 is required for nuclear pore complex assembly in vertebrate cells. Mol Cell 22, 93–103.
Martin-du Pan RC, Campana A (1993). Physiopathology of spermatogenic arrest. Fertil Steril 60, 937–946.
McNally FJ (2013). Mechanisms of spindle positioning. J Cell Biol 200, 131–140.
Ohkura H (2015). Meiosis: an overview of key differences from mitosis. Cold Spring Harb Perspect Biol 7.
Prasad R, Metherell LA, Clark AJ, Storr HL (2013). Deficiency of ALADIN impairs redox homeostasis in human adrenal cells and inhibits steroidogenesis. Endocrinology 154, 3209–3218.
Sarathi V, Shah NS (2010). Triple-A syndrome. Adv Exp Med Biol 685, 1–8.
Saskova A, Solc P, Baran V, Kubelka M, Schultz RM, Motlik J (2008). Aurora kinase A controls meiosis I progression in mouse oocytes. Cell Cycle 7, 2368–2376.
Schuh M, Ellenberg J (2008). A new model for asymmetric spindle positioning in mouse oocytes. Curr Biol 18, 1986–1992.
Schweizer N, Pawar N, Weiss M, Maiato H (2015). An organelle-exclusion envelope assists mitosis and underlies distinct molecular crowding in the spindle region. J Cell Biol 210, 695–704.
Schweizer N, Weiss M, Maiato H (2014). The dynamic spindle matrix. Curr Opin Cell Biol 28, 1–7.
Stavru F, Hulsmann BB, Spang A, Hartmann E, Cordes VC, Gorlich D (2006). NDC1: a crucial membrane-integral nucleoporin of metazoan nuclear pore complexes. J Cell Biol 173, 509–519.
Storr HL, Kind B, Parfitt DA, Chapple JP, Lorenz M, Koehler K, Huebner A, Clark AJ (2009). Deficiency of ferritin heavy-chain nuclear import in triple a syndrome implies nuclear oxidative damage as the primary disease mechanism. Mol Endocrinol 23, 2086–2094.
Touati SA, Cladiere D, Lister LM, Leontiou I, Chambon JP, Rattani A, Bottger F, Stemmann O, Nasmyth K, Herbert M, Wassmann K (2012). Cyclin A2 is required for sister chromatid segregation, but not separase control, in mouse oocyte meiosis. Cell Rep 2, 1077–1087.
Tullio-Pelet A, Salomon R, Hadj-Rabia S, Mugnier C, de Laet MH, Chaouachi B, Bakiri F, Brottier P, Cattolico L, Penet C, *et al*. (2000). Mutant WD-repeat protein in triple-A syndrome. Nat Genet 26, 332–335.
Verlhac MH, Lefebvre C, Guillaud P, Rassinier P, Maro B (2000). Asymmetric division in mouse oocytes: with or without Mos. Curr Biol 10, 1303–1306.
Yamazumi Y, Kamiya A, Nishida A, Nishihara A, Iemura S, Natsume T, Akiyama T (2009). The transmembrane nucleoporin NDC1 is required for targeting of ALADIN to nuclear pore complexes. Biochem Biophys Res Commun 389, 100–104.
Yeste M, Jones C, Amdani SN, Patel S, Coward K (2016). Oocyte activation deficiency: a role for an oocyte contribution? Hum Reprod Update 22, 23–47.
Yi K, Li R (2012). Actin cytoskeleton in cell polarity and asymmetric division during mouse oocyte maturation. Cytoskeleton 69, 727–737.
Zheng Y (2010). A membranous spindle matrix orchestrates cell division. Nat Rev Mol Cell Biol 11, 529–535.